JOURNAL OF NANO AND MATERIALS SCIENCE RESEARCH
Volume 3, No.1 (Special Issue, 2024), pp. 1 – 6
Available online at journals.nanotechunn.com/jnmsr

ORIGINAL ARTICLE

Study of the Morphological, Structural, Electrical, and Optical Features of Spray-Deposited Yttrium-doped Magnesium Selenide (YMgSe) Thin Film for Photovoltaic Applications

Ohiri C. Chidozie[a], Lebe A. Nnanna[a], Nwamaka I. Akpu[a,], Ugochukwu Joseph[a], Imosobomeh L. Ikhioya[b]*

[a]*Department of Physics, College of Physical and Applied Sciences, Michael Okpara University of Agriculture, Umudike, Abia State, Nigeria.*
[b]*Department of Physics and Astronomy, University of Nigeria Nsukka, 410001, Nigeria*

KEYWORDS

MgSe,
Yttrium,
Chalcogenide,
Spray pyrolysis,
Doping

ARTICLE HISTORY

Received: April 01, 2024
Revised: June 10, 2024
Accepted: July 16, 2024
Published: August 10, 2024

ABSTRACT

In this study, a spray pyrolysis approach was used to fabricate undoped and yttrium-doped magnesium selenide (0.01 – 0.04 mol%) chalcogenide materials. The deposited samples underwent comprehensive investigation, which covered analyses of their microstructure, elemental composition, structural, electrical, and optical properties with the aid of SEM cum EDX, XRD, four-point probe, and spectrophotometer accordingly. The micrograph results show that a high number of fine grains are well coated and distributed uniformly on the slide with their elemental composition analysis results confirming the formation of undoped and yttrium-doped MgSe. The undoped material's crystallinity decreased with the addition of the yttrium dopant. More so, hexagonal crystal structures with notable peaks were observed from the pattern for all the samples. From the electrical result, the resistivity and conductivity of the samples were seen to increase and decrease respectively with increasing film thickness which is one of the properties of a typical semiconductor material. The optical results show that yttrium-doped MgSe samples revealed improved features with an energy band gap ranging from 1.50 – 1.35 eV as compared to undoped MgSe with a value of 1.55 eV. The materials fabricated can be applied in the production of photovoltaic devices such as solar cells.

1 Introduction

In recent years, due to high activity of transition-metal chalcogenide semiconductors in water electro-catalysis have been widely utilized for improved energy-related applications [1]. They are largely famous for their desirable electronic and magnetic features. Significantly, the metal-chalcogen ratio in these transition metal chalcogenides may be altered over a vast range which can lead to subtle variations of their electronic features thereby providing opportunities for tuning such properties. Additionally, transition-metal selenides outperform transition-metal oxides in terms of electrochemical activity because oxygen has a larger electro-negativity than selenium. Consequently, substituting selenium with oxygen may yield a more adjustable microstructure [2]. Also, transition-metal selenides exhibit significantly higher electrical conductivity than metal oxides/sulfides [2] – [5]. Therefore, transition-metal selenides just like CoSe [6],[7], CdSe [2],[3], CuSe [8],[9], MgSe [10],[11], FeSe [12], MnSe [13] and ZnSe [14],[15] are required to display good electro-chemical and optical features for usage as electrode-active materials, thermoelectric, and absorber layer in solar energy collection [5].

Among the numerous metal selenide thin materials, Magnesium selenide (MgSe) is specifically an attractive group II – IV semiconductor binary family, which can exist in various phases [11], such as rock salt, wurtzite, and zinc blende with an experimental lattice constant of 5.89 and wide band gap of

* **CORRESPONDING AUTHOR** | N. I. Akpu, ✉ akpu.nwamaka@mouau.edu.ng

4 eV at 0 K. MgSe has been widely used for different purposes ranging from microelectronics, photoelectric devices, and solar selective coating down to catalysis [5]. More so, due to its wide band gap, it can be used in devices capable of operating at high-power levels, high-temperature, and ultraviolent wavelength optics as in light emitting diodes (LEDs) and cladding materials for ZnSe-based laser diodes [11].

Doping is the purposeful introduction of impurities into an intrinsic semiconductor during its manufacturing to modify its electrical, optical, and structural properties [8]. However, to improve the photovoltaic performance of most of these metal chalcogenides, various researchers introduced impurities that positively altered some of the properties of these thin films in question [6], via supporting, coupling, and doping of these compounds. Rare earth-doped nano-particles have received so much consideration because of their large oxygen vacancy content, huge photocatalytic activity in the degradation of organic contaminants due to electron–hole recombination suppression, and strong absorption of hydroxide ions on the catalyst's surface [8]. They are also seen to execute helpful activities which include stabilizing and lowering the dissipation factor in dielectric materials due to their low diffusivity.

Yttrium (Y^{3+}) is one of the most promising rare earth dopants. This is because it increases fatigue endurance, remanent polarization, and leakage current [8]. Yttrium can also function as an acceptor or donor ion. Another important impact of yttrium incorporation is the modification in the electrical conductivity of the doped material with respect to the doping location. Moreover, there is currently no published article on yttrium-doped MgSe thin film.

Various synthesis techniques such as spray pyrolysis, thermal evaporation, MOCVD, Chemical vapor deposition, and chemical bath have been employed in the fabrication of nano-sized MgSe having unique features for numerous applications [16] – [23]. Ubale et al. studied the structural, electrical, and optical properties of chemically deposited MgSe thin materials. The effect of varied quantities of triethanolamine as a complexing agent in the deposition bath was studied and the outcome shows that an increase in the triethanolamine in the deposition bath led to a decline in the optical bandgap and electrical resistivity of the films [20].

Ubale and Sakhare investigated the thickness-dependent physical characteristics of nanocrystalline MgSe thin films formed at room temperature using the solution growth deposition technique. The result reveals that the XRD increases with thickness while the optical band-gap and electrical resistivity of MgSe decreases as the film thickness increases. The SEM results reveal a uniform distribution of the MgSe thin material over the entire substrate surface which is similar to the result obtained in this current study [22]. Alharbi and Qasrawi studied the effect of substrate type on MgSe. A semi-transparent indium thin films with a thickness of 200 nm were used as substrate for depositing MgSe thin films. Using a vacuum pressure of 10^{-5} mbar, both indium and MgSe films were coated onto ultrasonically cleaned glass substrates. The morphological and structural studies on these thin films showed that indium conducting layers suppressed the formation of cubic $MgSe_2$ phase in the films. The indium (In) substrate was observed to improve the light absorption, resulting in a shift in the direct allowed transitions band gap from 2.54 eV to 1.92 eV [23]. Algami et al. did similar work with semi-transparent platinum substrates using a vacuum evaporation technique under the same vacuum pressure of 10^{-5} mbar. The platinum nanosheet substrate was also found to enhance the optical, electrical, and structural features of MgSe [17]. Sakhare et al. reported the influence of the quantity of spray solution on the electrical, structural, optical features, and microstructure of spray-deposited nanocrystalline MgSe thin film. XRD studies revealed cubic lattice, a direct optical band gap which ranges from 2.45 to 2.75 eV. The electrical resistivity of MgSe decreased with an increase in temperature denoting a semiconducting nature. More so, the resistivity, optical band gap, and activation were seen to depend upon the quantity of spray solution [18].

This study utilized the spray pyrolysis deposition process. It has numerous notable benefits, including the flexibility to vary the film's properties by changing the composition of the starting material, i.e., adding dopants and modifying the film morphology, as well as reducing production costs when large-scale fabrication is needed. It is a pretty inexpensive and straight forward procedure. Spray-fabricated materials are used in a wide range of applications, including anti-reflective coatings, optoelectronic devices, sensors, etc. [9]. More so, in this research, the core focus is on the influence of yttrium dopant on MgSe. To investigate how this yttrium dopant will enhance the microstructure, composition, structural features, optical properties, and electrical features of MgSe for better application in the production industry.

2 Experimental Report

2.1 Materials Used

The materials used in this research were bought from Sigma Aldrich, which includes magnesium acetate hydrate [$Mg(CH_3COO)_2.4H_2O$], selenium (IV) oxide (SeO_2), yttrium (Y), hydrogen chloride (HCl), deionized water, soda lime, a glass substrate, and a spray machine. For the substrate cleaning procedure, acetone and methanol were used.

2.2 Deposition of Y_xMgSe (x = 0, 0.01, 0.02, 0.03 and 0.04 mol%) nanomaterial

For the calculation of the yttrium (Y) doping concentration in mol%, Equation 1 [15] was used.

$$\%\text{doping} = \frac{x\% \times \text{molarity}\left(\frac{\text{mol}}{\text{dm}^3}\right) \times \text{molar mass}\left(\frac{\text{g}}{\text{mol}}\right) \times \text{Volume}\left(\text{dm}^3\right)}{1000} \quad (1)$$

For the Mg^+ ion, 0.01 mol solution of magnesium acetate ($Mg(CH_3COO)_2.4H_2O$) with a molecular weight of 214.46 g was prepared by dissolving 1.28 g in 500 ml of deionized H_2O. While, for the Se^+ ion, 0.01 solution of selenium (IV) oxide

(SeO_2) with a molar weight of 78.96 g was prepared by dissolving 3.158 g with 5 ml of hydrogen chloride (HCl) and 100 ml of deionized water. Before the deposition, these glass substrates were first cleaned with water, immersed in acetone and methanol for 24 hours, and rinsed with deionized water. Afterward, they were cleaned ultrasonically for 30 minutes, rinsed, and allowed to air dry.

Using the spray pyrolysis machine, the precursor (MgSe) ion is pumped via the pump directly to the nozzle, as the mixture gets to the substrate through the nozzle and hits the surface of the substrate, evaporation of the residual solvent takes place, spreading of the droplet and then the salt decomposition. Via this procedure, MgSe material is deposited on the substrate. Film uniformity is achieved by moving the nozzle.

This process was repeated with a doping agent, yttrium (Y) at different doping molar percentages (0.01, 0.02, 0.03, and 0.04 mol%). The spray process also includes the optimization of various process parameters such as 0.07 ml/min flow rate, outside and internal diameter of 0.32 and 0.16 mm respectively, 8 mm spray nozzle to substrate distance, 3.5 kV atomizing voltage, and a constant temperature of 400 ℃. Table 1 displays the deposition parameters of Y_xMgSe (x = 0, 0.01, 0.02, 0.03 and 0.04 mol%) nanomaterial.

2.3 *Characterization of Y_xMgSe (x = 0, 0.01, 0.02, 0.03 and 0.04 mol%) nanomaterial*

The Y_xMgSe (x = 0, 0.01, 0.02, 0.03, and 0.04 mol%) material morphological features and elemental composition were ascertained with the aid of Scanning electron microscopy (SEM)/Energy dispersive X-ray spectroscopy (EDX). The structural properties were characterized using X-ray diffractometry, while the electrical and optical property characterizations were obtained using a Janel four-point probe and spectrophotometer accordingly.

Table 1: Deposition parameters of Y_xMgSe (x = 0, 0.01, 0.02, 0.03 and 0.04 mol%) nanomaterial

Sample	Sample code	Mg $(CH_3COO)_2.4H_2O$ (ml)	SeO_2 (ml)	Yttrium (ml)	Voltages (kV)	Dopant conc. (yttrium) (mol%)
MgSe	MG	20	10		3.5	
$Y_{0.01mol\%}$MgSe	MGY (0.01)	20	10	5	3.5	0.01
$Y_{0.02mol\%}$MgSe	MGY (0.02)	20	10	5	3.5	0.02
$Y_{0.03mol\%}$MgSe	MGY (0.03)	20	10	5	3.5	0.03
$Y_{0.04mol\%}$MgSe	MGY (0.04)	20	10	5	3.5	0.04

Table 2: Structural properties for the MgSe and Yttrium-doped MgSe

Sample	2θ (degree)	Spacing, d (Å)	Lattice constant, a (Å)	FWHM, β	hkl	Crystallite Size, d (nm)	Dislocation density, δ (m^2)
MG-MgSe	15.1903	5.8272	10.0930	0.18517	111	0.7554	5.3132
	19.8909	4.4594	8.91898	0.20958	200	0.6716	6.7321
	23.0818	3.8490	7.69942	0.1480	201	0.9561	3.3223
	30.0126	2.9746	6.65143	0.22584	210	0.6375	7.4478
	46.6533	1.9450	4.76449	0.22499	211	0.6711	6.7067
	63.7401	1.4587	4.12596	0.19652	300	0.8308	4.3453
MGY-YMgSe	11.0044	8.0326	13.9129	0.18517	111	0.7523	5.3579
	15.1903	5.8272	11.6544	0.20958	200	0.6674	6.8178
	23.0475	3.8553	7.7107	0.1480	201	0.9561	3.3227
	30.6302	2.9160	6.5204	0.22584	210	0.6365	7.4261
	46.8592	1.9370	4.7447	0.22499	211	0.6716	6.6963
	51.5598	1.7709	5.0089	0.19652	300	0.7835	4.8853

3 Results and Discussions

3.1 *SEM/EDX results of Y_xMgSe (x = 0, 0.01, and 0.04 mol%) nanomaterial*

The SEM imagery shown in Figure 1(a–c) depicts the morphological details of MgSe and yttrium-doped MgSe (0.01 and 0.04 mol%). A well-distributed, homogenous, and densely packed film on the substrate surface was observed. The undoped MgSe sample showed a nanoflake structure that got transformed into a nanorod structure upon the addition of a lower concentration of yttrium dopants (0.01 mol%).

For a higher concentration of yttrium dopant (0.04 mol%), the morphological nature of MgSe was not altered instead a more coalescence surface was obtained. The surface pattern obtained after doping with a lower concentration of yttrium allowed easy

transmission of light upon incidence on the film surface [3], [24].

EDX was used to ascertain the elemental composition of the undoped, and yttrium-doped deposited films as shown in Figure 2(a–b). The spectrum depicts the basic elements, which include magnesium, selenium, and yttrium. The undoped samples have different compositions from the doped samples.

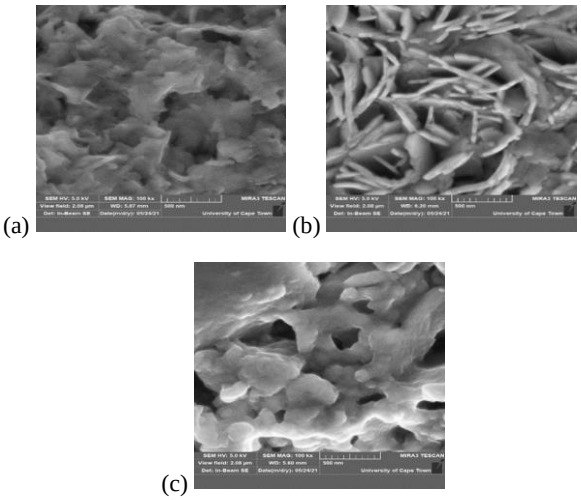

(a) (b) (c)

Figure 1: a) MG control b) MGY 0.001 mol% c) MGY 0.004 mol% microstructural image of Y_xMgSe [x = a)0, b) 0.01 and c) 0.04 mol%)]

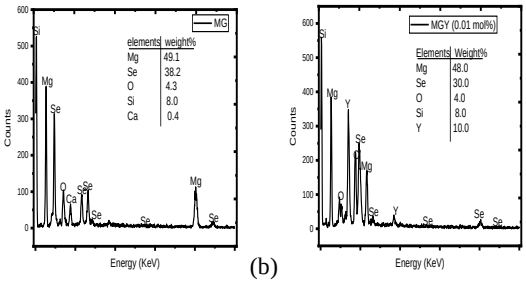

(a) (b)

Figure 2: EDX graph of Y_xMgSe [x = a) 0, b) 0.01 mol%]

3.2 *XRD results of Y_xMgSe (x = 0, 0.01, 0.02, 0.03 and 0.04 mol%) nanomaterials*

Figure 3 shows the XRD result of Y_xMgSe (*x* = 0, 0.01, 0.02, 0.03 and 0.04 mol%) nanomaterials. All the samples have polycrystalline structure of hexagonal phase due to the numerous peaks, but with a preferred orientation along the (210) for undoped MgSe and (201) for all the yttrium doped MgSe irrespective of dopant concentration. The presence of high peaks is important as it creates a large surface area for effective photovoltaic activities [25].

Doping MgSe films with yttrium declined the crystallinity as seen in Figure 3 from the decreased peak intensity at increasing dopant mol%. This result corresponds to the low absorbance value obtained from the optical result. The results obtained during XRD study was used in calculating some other structural parameters [25] – [29] of undoped and Y-doped MgSe such as crystallite size (D), interplanar spacing (d), dislocation density (δ), and lattice constant (a) that were obtainable using Equations 2–5 and outlined in Table 1.

$$D = {k\lambda}/{\beta\cos\theta} \quad (2)$$

$$d = {\lambda}/{2\sin\theta} \quad (3)$$

$$\delta = {1}/{D^2} \quad (4)$$

$$a = d\sqrt{h^2 + k^2 + l^2} \quad (5)$$

Where k = 0.94, λ = wavelength of the X-ray source given as 0.154 nm, θ = the Bragg's angle/diffraction angle.

From Table 2, the crystallite size and FWHM were seen to be inversely proportional. As the FWHM angle increases the crystallite size decreases and vice versa. No particular trend was observed. More so, the position of the peaks and the lattice constant (a), was significantly altered upon the introduction of the yttrium dopant. This corresponds to the morphology result obtained in this work.

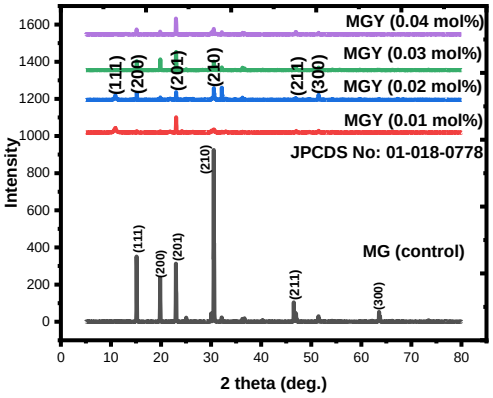

Figure 3: X-ray diffraction (XRD) result of MgSe and yttrium-doped MgSe at different molar percentage dopant

3.3 *Electrical characterization of Y_xMgSe (x = 0, 0.01, 0.02, 0.03 and 0.04 mol%) nanomaterials*

The electrical characterization of Y_xMgSe (*x* = 0, 0.01, 0.02, 0.03, and 0.04 mol%) nanomaterials are shown in Table 3. The addition of the yttrium dopant grew the thickness of the yttrium-doped MgSe from 164.01 to 198.03 nm. Figure 4 demonstrates how resistivity and conductivity increase and decrease respectively with increasing film thickness which is one of the properties of a typical semiconductor material [6]. The improved resistivity of fabricated materials enables the development of promising solar device materials [25].

Table 3: Electrical properties of Y_xMgSe (x = 0, 0.01, 0.02, 0.03 and 0.04 mol%) nanomaterials

Sample code (mol%)	Thickness, t (nm)	ρ (Ω.m) × 10^{-4}	σ (Ω.m)$^{-1}$ × 10^{-3}
MG	164.01	4.132	2.420
MGY (0.01)	172.05	4.276	2.338
MGY (0.02)	176.07	4.321	2.314
MGY (0.03)	182.02	4.421	2.261
MGY (0.04)	198.03	4.511	2.216

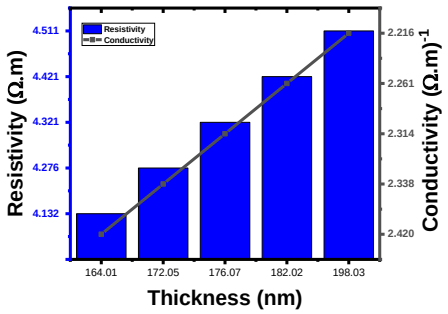

Figure 4: Bar chart comparison of conductivity and resistivity of Y_xMgSe (x = 0, 0.01, 0.02, 0.03 and 0.04 mol%) nanomaterials with film thickness

3.4 *Optical analysis of Y_xMgSe (x = 0, 0.01, 0.02, 0.03 and 0.04 mol%) nanomaterials*

Figure 5(a–d) illustrates (a) the absorbance (b) the transmittance (c) the reflectance and (d) the energy band gap values of Y_xMgSe (x = 0, 0.01, 0.02, 0.03, and 0.04 mol%) nanomaterials. Figure 5a shows that the absorbance value for undoped MgSe has a constant value almost all through the spectrum while yttrium-doped samples decreased as the wavelength tends toward the VIS-IR region. MgSe doped with 0.03 mol% of yttrium recorded the highest absorbance value all through the spectrum with an average maximum value of 2.5 at the ultraviolet region, followed by 0.04 mol% yttrium doped MgSe, undoped MgSe, MgSe doped with 0.02 mol% and 0.01 mol% of yttrium respectively.

Following this trend of increase, we observed that the incorporation of a higher concentration of yttrium was seen to increase the absorbance value of pure MgSe. A similar result was reported by Lohar et al., for electrodeposited iron-doped ZnSe [30], and a decreasing trend with respect to high wavelength was also reported by Jeroh et al., for Eu-doped CdSe deposited by spray pyrolysis [31]. The addition of dopant resulted in a decline in the absorbance spectra.

The explanation behind this could be attributed to the observed decrease in the crystallite peak in the XRD pattern, followed by a decrease in the size of the crystallites after adding the yttrium dopant. More so, the high absorbance exhibited by these films (especially undoped and 0.03 mol% Y doped MgSe) in the near-infrared and visible region of the spectrum makes them suitable material for p-n junction formation in solar cells as well as photovoltaic purposes in general [32].

The transmittance values are as shown in Figure 5b and evaluated from the absorbance values using Equation 6 [32]:

$$T = 10^{-A}. \quad (6)$$

$$R = 1 - (A + T). \quad (7)$$

where A=Absorbance, T=Transmittance, and R=Reflectance.

Here, it reveals that the undoped MgSe has a very low transmittance value which was greatly improved when doped with yttrium especially in the VIS-IR region of the spectrum thereby making yttrium doped MgSe an interesting material for the production of photovoltaic device. All the samples were observed to exhibit relatively low transmittance value (> 40%) in the ultra-violet region while MgSe doped with 0.01 mol% of yttrium recorded the highest transmittance with an average value of 60% in the visible and near infra-red region. From our findings, no researcher has grown MgSe doped with yttrium (YMgSe).

From the reflectance values as shown in Figure 5c, evaluated using Equation 7 [33], all the deposited films exhibited very low reflectance values but the introduction of yttrium dopant on MgSe increases the values. More so, the reflectance value was seen to increase slightly from the ultraviolet to the visible region and was almost constant throughout the visible and near infra-red region with a maximum value of > 0.3 for all the deposited films. The low reflectance value, especially in the visible region, makes them good material for anti-reflective coating and solar control coating in photovoltaic applications [32].

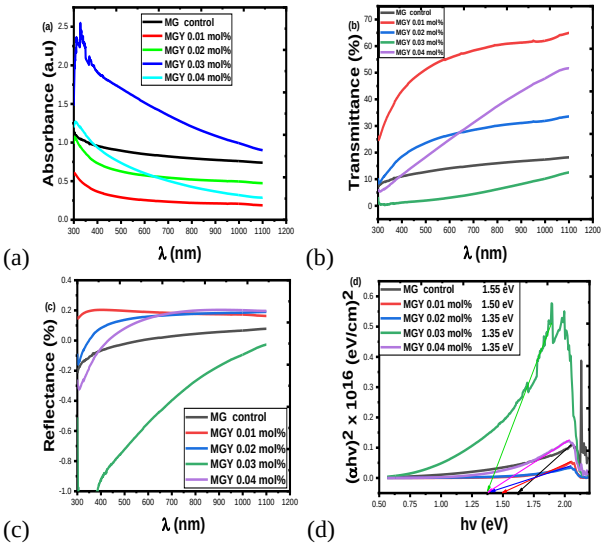

Figure 5: a) Absorbance b) Transmittance c) Reflectance d) $(\alpha h\upsilon)^2$ against photon energy ($h\upsilon$) plots of Y_xMgSe (x = 0, 0.01, 0.02, 0.03 and 0.04 mol%) nanomaterials

Figure 5d depicts the relationship between $(\alpha h\upsilon)^2$ and $h\upsilon$ for undoped and yttrium-doped MgSe at different dopant concentrations. The energy band gaps for undoped and Y-doped MgSe at different dopant concentrations were estimated from the graph in Figure 5d by extrapolation of the straight portion of the graph down to $h\upsilon$ axes at $(\alpha h\upsilon)^2 = 0$ [32],[33]. The energy band gaps of the deposited films were found to be within the range of 1.35 eV to 1.55 eV. The introduction of yttrium as a dopant resulted in a decrease in the energy band gap, E_g, and further decreased as the yttrium concentration increased. Thus, Y dopant was found to improve the energy band gap of MgSe.

Similar results in the energy band gap, E_g for doped films were reported for electrochemically deposited Yb-ZnO [28] and Yb-ZrSe [34] thin films. The E_g range obtained in this study is good

for the absorber layer in solar cells because it will absorb all solar energy radiation greater than 1.35 eV and theoretically it matches well with the sun's maxima spectrum (band gap ~1.5 eV).

4 Conclusions

Magnesium selenide and yttrium doped magnesium selenide (Y_xMgSe; x = 0, 0.01, 0.02, 0.03, and 0.04 mol%) nanomaterials have been successfully synthesized from magnesium acetate hydrate [Mg $(CH_3COO)_2.4H_2O$], selenium (IV) oxide (SeO_2) and hydrogen chloride (HCl), yttrium (Y), using a spray pyrolysis deposition technique. The deposited samples underwent comprehensive investigation, primarily to ascertain the effect of yttrium dopant concentration on MgSe, which covered analyses of their microstructure, elemental composition, structural, electrical, and optical properties with the aid of SEM/EDS, XRD, four-point probe, and spectrophotometer respectively. From the findings, a well-distributed, homogenous, densely packed, and agglomerated grain film on the substrate surface was observed for all the samples. At closer observation, MgSe doped with 0.01 mol% of yttrium gave a more pronounced and well-defined microstructure when compared to the undoped and 0.04 mol% yttrium doped samples. The microstructure result indicates uniform deposition, and the film cells can serve as a good material for photovoltaic devices. The elemental composition analysis results confirm the formation of undoped and yttrium-doped MgSe due to the presence of all the basic elements (Mg, Se, and Y). For the XRD, the result reveals that all the samples possess a hexagonal crystal structure with notable peaks. The effect of the yttrium dopant was also evident because the undoped MgSe material had a better crystallinity which decreased after incorporating the yttrium dopant. From the electrical result, the resistivity and conductivity of the samples were seen to increase and decrease respectively with increasing film thickness which is one of the basic properties of typical semiconductor material. The optical properties of undoped MgSe were enhanced when the yttrium dopant was added. The yttrium dopant narrowed the band gap energy of undoped MgSe from 1.55 eV to a range of 1.50 – 1.35 eV. Samples with higher concentrations of yttrium (0.02 – 0.04 mol%) recorded the least band gap thereby making the yttrium-doped MgSe a better Material for the production of photovoltaic devices such as solar cells among others.

Acknowledgment

We appreciate the immense contribution of all the authors to the success of the research.

Authors' Credit Statement

Ohiri C. Chidozie, Lebe A. Nnanna, Imosobomeh L. Ikhioya, Nwamaka I. Akpu, Ugochukwu Joseph, conceptualization, methodology, data analysis, graphical plots, writing of original draft; **Imosobomeh L. Ikhioya, Nwamaka I. Akpu, Ugochukwu Joseph,** editing, proofreading and manuscript handling; **Imosobomeh L. Ikhioya, Nwamaka I. Akpu, Lebe A. Nnanna**: supervision and suggestions.

Declaration of Competing Interest

The authors declare no personal or financial conflicts that may influence the research presented in this paper.

References

[1] J. Masud, A. Swesi, W. P. R Liyanage, & M. Nath, "Cobalt Selenide Nanostructures: An Efficient Bifunctional Catalyst with High Current Density at Low Coverage", ACS Applied Materials and Interfaces 8 (2016) pp.17292-17302. DOI: 10.1021/acsami.6b04862

[2] N. I Akpu, M.O Akpu, Onwuzo C. Julia & I. L. Ikhioya, "Growth and optimization of physical properties of cadmium selenide semiconductor material via yttrium doping for photovoltaic/solar energy purposes", J. Mater. Environ. Sci., 13 (2022) Pp. 681-691. http://www.jmaterenvironsci.com

[3] N. I. Akpu, A. D Asiegbu, L.A Nnanna, & I. L. Ikhioya," Investigation on The Influence of Varying Substrate Temperature on The Physical Features of Yttrium Doped Cadmium Selenide Thin Films Materials", SSRG International Journal of Applied Physics 8 (2021) 37-46, doi:10.14445/23500301/ IJAP-V8I2P106

[4] X. Zhang, J. Gong, K. Zhang, W. Zhu, Jing-chang Li, & Q. Ding, "All-Solid-State Asymmetric Super Capacitor Based on Porous Cobalt Selenide Thin Films", Journal of alloys and compounds. 772 (2019) 25 – 32. https://doi.org/10.1016/j.jallcom.2018.09.023

[5] S. J. Gnanamuthu, S. J. Jeyakumar, A. R. Balu, K. Usharani & V. S. Nagarethinam, Characteristic Analysis on the Physical Properties of Nanostructured MgSe Thin Films – Substrate Temperature Effect. Int. J. Thin. Fil. Sci. Tec. 4 (2015) pp121-123. http://dx.doi.org/10.12785/ijtfst/040209

[6] N. I. Akpu, K. U. P. Okpechi, E. C. Nwaokorongwu, I. L. Ikhioya, J. C. Onwuzo, L. A. Nnanna & I. I.C Agbodike, "Impact of temperature difference on the features of spray deposited yttrium doped cobalt selenide (YCoSe) thin film for photovoltaic application", African Scientific Reports 2 (2023) 143. DOI:10.46481/asr.2023.2.3.143

[7] I. L. Ikhioya, G. M. Whyte, & A. C. Nkele, "Temperature-modulated nanostructures of ytterbium-doped Cobalt Selenide (Yb-CoSe) for photovoltaic application", Journal of the Indian Chemical Society 100(2023) 100848. https://doi.org/10.1016/j.jics.2022.100848

[8] N .I. Akpu, A. D. Asiegbu, L. A Nnanna, IL Ikhioya, & T. C. Mgbeojedo, "Synthesis and characterization of novel yttrium- incorporated copper selenide (CuSe:Y)

thin materials for solar energy applications", Mater Sci: Mater Electron, 33 (2022) 1154–116, https://doi.org/10.1007/s10854-021-07397-x

[9] N. I. Akpu, A. D. Asiegbu, L. A Nnanna, IL Ikhioya, & T. C. Mgbeojedo, "Influence of Substrate Temperature on the Photovoltaic/ Optoelectronic properties of Spray Synthesized Yttrium Copper Selenide (YCS) Thin Films", Arabian Journal for Science and Engineering, 47 (2022) 7639–7646. https://doi.org/10.1007/s13369-021-06455-0

[10] R. A. Almotiri & A. F. Qasrawi, "ITO/MgSe interfaces designed as gigahertz/terahertz filters" Physica Scripta, 98 (2023) 045806. DOI 10.1088/1402-4896/acbb3a.

[11] Z. Bordjiba , A. Meddour, & C. Bourouis, "Ab Initio Theoretical Prediction of Structural, Electronic, and Magnetic Properties in the 3d (Mn)-Doped Zinc-Blende MgSe: A DFT-mBJ Approach" J Supercond, 31 (2018) 2261-2270. https://doi.org/10.1007/s"10948-017-4495-5

[12] F. Lan, Z. Ma, Y. Liu, Ning Chen, Qi Cai, Huijun Li, ShaonBarua, Dipak Patel, M. Shahriar Al Hossain, Jung Ho Kim & Shi Xue Dou, "The formation of nano-layered grains and their enhanced superconducting transition temperature in Mg-doped FeSe0.9 bulks", Scientific Reports, 4 (2014) 6481. DOI: 10.1038/srep06481

[13] İ. A. Kariper, "A New Route to Synthesize MnSe Thin Films by Chemical Bath Deposition Method", Materials Research. 21(2018) 20170215. http://dx.doi.org/10.1590/1980-5373-MR-2017-0215

[14] I. L. Ikhioya, E. Danladi, D. N. Okoli & A. O. Salawu, "Influence of Precursor Temperature on Bi-Doped ZnSe Material via Electrochemical Deposition Technique for Photovoltaic Application" Journal of the Nigerian Society of Physical Sciences 4 (2022) 129. https://doi.org/10.46481/jnsps.2022.502

[15] B.C.N. Obitte, I.L. Ikhioya, G.M. Whyte, U.K. Chime, B.A. Ezekoye, A.B.C. Ekwealor, M. Maaza, & Fabian I. Ezema, "The effects of doping and temperature on properties of electrochemically deposited Er3+ doped ZnSe thin films", Optical Materials 124 (2022) 111970. https://doi.org/10.1016/j.optmat.2022.111979

[16] R. A. Almotiri & A. F. Qasrawi, "Optoelectronic performance of n-Si/p-MgSe heterojunctions as a visible light communication component" Optik, 271 (2022) 170106. https://doi.org/10.1016/j.ijleo.2022.170106

[17] S. E. Algarni, A. F. Qasrawi, & N. M. Khusayfan, "Enhanced Optical and Electrical Interactions at the Pt/MgSe Interfaces Designed for 6G Communication Technology", Crystal Research and Technology, 58 (2022) 2200185. https://doi.org/10.1002/crat.202200185.

[18] Y. S. Sakhare, Nilesh R. Thakare, & Ashok U. Ubale, "Influence of quantity of spray solution on the physical properties of spray deposited nanocrystalline MgSe thin film', Physics and Mathematics 2 (2016) 17–26. http://dx.doi.org/10.1016/j.spjpm.2016.01.005

[19] A. U. Ubale & Y. S Sakhare, "Growth of nanocrystalline MgSe thin films by spray pyrolysis", Vacuum, 99: 124– 126, (2014). https://doi.org/10.1016/j.vacuum.2013.05.004

[20] A. U. Ubale, Y.S Sakhare, Bhute M.V, Belkhedkar M. R, & Sing A. "Structural, optical and electric properties of nanocrystalline MgSe thin films deposited by chemical route using triethanolamine as a complexing agent", Solid State Sci, 16 (2013) 134–139. https://doi.org/10.1016/j.solidstatesciences.2013.05.016

[21] J. Fengyi, L. Qinghua, F. Guanghan, X. Huanbing, P. Xuexin, P. Chuankang, & L. Nianhua, "MOCVD growth of MgSe thin films on GaAs substrates", Journal of Crystal Growth. 183 (1998) pp 289 – 293. https://doi.org/10.1016/S0022-0248(97)00426-0

[22] A. U. Ubale &Y.S. Sakhare, "Thickness dependent physical properties of chemically deposited nanocrystalline MgSe thin films deposited at room temperature by solution growth method", Materials science in semiconductor processing 16 (2013) pp 1769- 74. https://doi.org/10.1016/j.mssp.2013.06.015

[23] S. R. Alharbi & A. F Qasrawi, "In/MgSe Terahertz Filters with Enhanced Optical Conduction and Light Absorption. J. Electron. Mater., 52 (2023) 3613–3621. Https://doi.org/10.1007/s11664-023-10351-8

[24] I. L. Ikhioya, D. N. Okoli, & A. J. Ekpunobi, "Effect of Temperature on SnZnSe Semiconductor Thin Films for Photovoltaic Application', SRG International Journal of Applied Physics (SSRG-IJAP), 6 (2019) pp 55 – 67. www.internationaljournalssrg.org

[25] I. L. Ikhioya, N. I Akpu, E. U Onoh, S. Olatubosun Aisida, Ishaq Ahmad, M. Maaza, & F. I. Ezema, Impact of precursor temperature on physical properties of molybdenum doped nickel telluride metal chalcogenide material. Asian Journal Nanoscience and Materials 2 (2023) 156-167. DOI: 10.26655/AJNANOMAT.2023.2.5

[26] I. L. Ikhioya, Nwamaka I. Akpu, Edwin U. Onoha, S. O. Aisida, I Ahmad, M. Maaza, & F. I. Ezema, Enhanced physical properties of nickel telluride metal chalcogenide material with molybdenum dopant. Materials Research Innovations. 2023 https://doi.org/10.1080/14328917.2023.2222465

[27] I. L. Ikhioya, N. I. Akpu, & F. U. Ochai-Ejeh, "Influence of erbium (Er) dopant on the enhanced optical properties of electrochemically deposited zinc oxide (ZnO) films for high-performance photovoltaic systems", Optik - International Journal for Light and Electron Optics 252 (2022) 168486. https://doi.org/10.1016/j.ijleo.2021.168486

[28] I. L Ikhioya, N. I Akpu & A. C Nkele "Influence of ytterbium (Yb) dopant on the optical properties of electrochemically deposited zinc oxide (ZnO) films", Mater. Res. Express 8 (2021) 016403. https://doi.org/10.1088/2053-1591/abd5d6

[29] J. C. Osuwa & N. I. Chigbo, "Characterization of structural and electrical properties of electro-deposited cadmium telluride (CdTe) thin films at varying deposition time on glass FTO", Chalcogenide Letters, 9 (2012) 501 – 508. https://www.researchgate.net/publication/287586583

[30] G.M Lohar, J.V Thombare, S.K Shinde, U.M Chougale & V. J. Fulari, "Preparation and Characterization Iron doped Zinc Selenide Thin Film by Electrodeposition. Journal of Shivaji University (Science & Technology). 41 (2015) pp 1-3. https://www.unishivaji.ac.in/journals/Stech-Volume-No-41(2)-2014-15

[31] M. D. Jeroh, A. J. Ekpunobi & D.N. Okoli, "Optical analytical studies of Electrostatic sprayed Eu-doped Cadmium selenide nanofilms at different temperatures". Journal of nano and electronic physics, 10(2018) 03006. https://doi.org/10.21272/jnep.10(3).03006

[32] N. I Akpu, C. A. Sylvanus, E. C. Nwaokorongwu, I. L. Ikhioya, E. O. Okechukwu, L. U. Ugwu, & A. J. Ekpunobi, Modulation of the physical properties of spray-deposited cobalt selenide nanofilm via yttrium doping for photovoltaic purposes. J. Mater. Environ. Sci., 2023, Volume 14, Issue 11, Page 1230 1244. http://www.jmaterenvironsci.com

[33] E. C. Nwaokorongwu, N. I. Akpu. & J. Ugochukwu Growth and Optical Characterization of Copper Sulphide Thin Films by Sol-Gel Technique. International Journal of Innovative Scientific & Engineering Technologies Research 6(2):38-44, 2018. www.seahipaj.org

[34] L. I Ikhioya, U. K. Chime, C. F Okoro, C. Iroegbu, M. Maaza, & Fabian I Ezema, "Influence of dopant concentration on the electronic band gap energy of Yb-ZrSe2 thin films for photovoltaic application via electrochemical deposition technique, Mater. Res. Express 7 (2020) 026420 https://doi.org/10.1088/2053-1591/ab7690